

Electronic Supplementary Information

Highly Efficient and Low Voltage Silver Nanowire- Based OLEDs employing n-Type Hole Injection Layer

Hyungjin Lee,^a Donghwa Lee,^a Yumi Ahn,^a Eun-Woo Lee,^b Lee Soon Park,^c and Youngu Lee^{*a}

**correspondence to : youngulee@dgist.ac.kr*

^aDepartment of Energy Systems Engineering, Daegu Gyeongbuk Institute of Science and Technology (DGIST), 50-1 Sang-Ri, Hyeonpung-Myeon, Dalseong-Gun, Daegu, 711-873, Korea

^bDisplay Nanomaterials Institute (DNI), Kyungpook National University, 1370 Sankyuk-Dong, Buk-Ku, Daegu, 702-701, Korea

^cDepartment of Materials Science and Engineering, Ulsan National Institute of Science and Technology (UNIST), UNIST-gil 50, Ulsan, 689-798, Korea

Preparation of AgNWs TCE

Substrates were cleaned using acetone, deionized water, and isopropyl alcohol. They were treated with UV-ozone for 20 min to obtain a hydrophilic surface. Then, a AgNWs (Cambrios Technologies Corporation) ink was spin-coated onto the cleaned substrates. The spin-coated AgNWs ink was then dried at 120 °C for 5 min to obtain a AgNWs TCE.

Characterization of AgNWs TCEs

The optical transmittance of AgNWs and ITO TCEs was measured by using a UV/Vis/NIR spectrophotometer (CARY 5000 spectrophotometer, Agilent). The sheet resistance of both samples was measured by using a non-contact sheet resistance measurement instrument (EC-80, Napson). Figure S1 shows optical transmittance of AgNWs TCEs as a function of wavelength. As spin rate increases, optical transmittance and sheet resistance of AgNWs TCEs tend to increase.

Mechanical flexibility tests of AgNWs and ITO TCEs

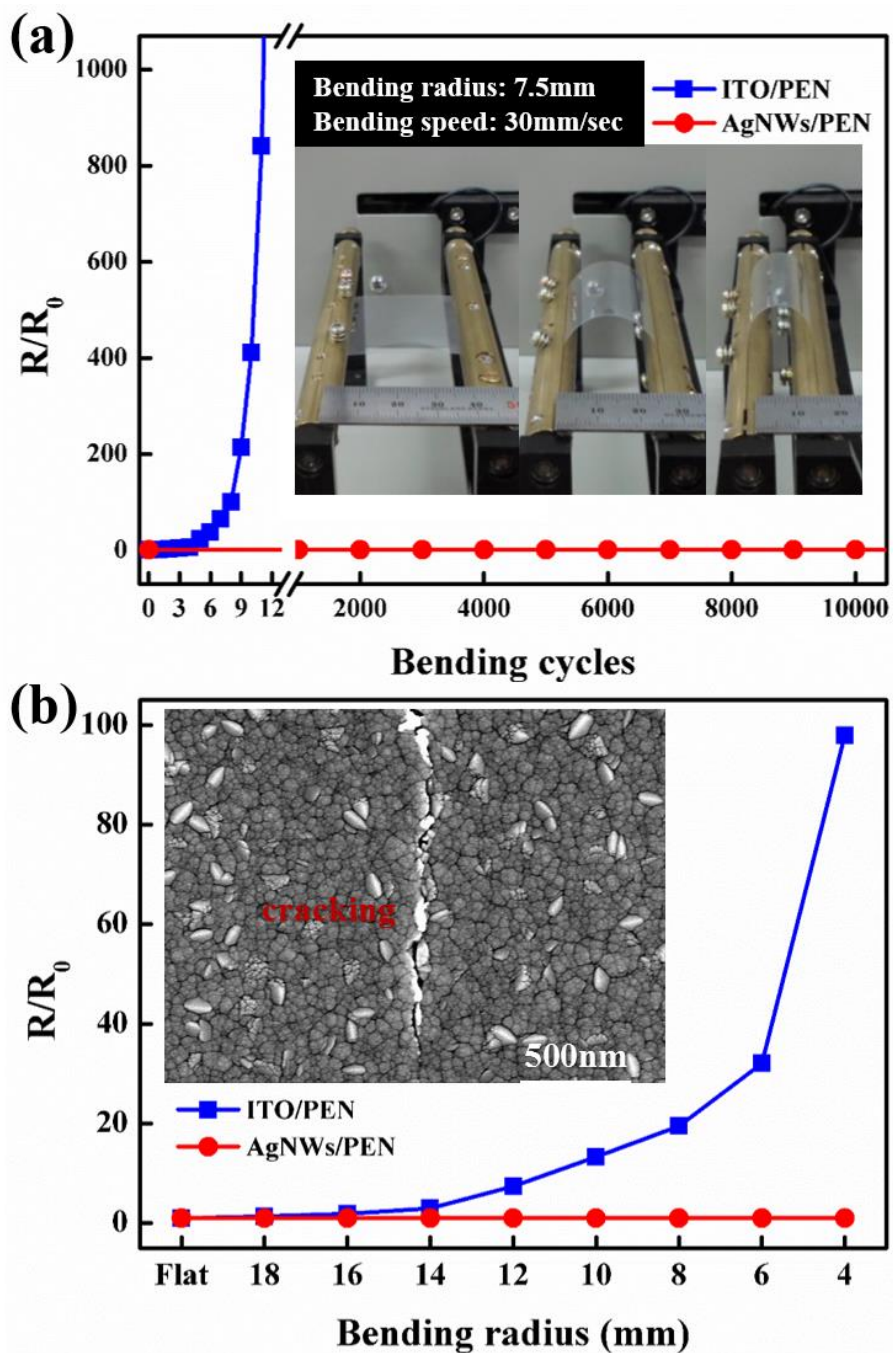


Fig. S1 The mechanical flexibility test of ITO/PEN and AgNWs/PEN TCEs by (a) bending cycles and (b) bending radius, Inset: The SEM image of ITO/PEN TCE after mechanical flexibility test.

Mechanical flexibility tests of ITO/PEN and AgNWs/PEN TCEs ($40 \times 40 \text{ mm}^2$) were performed using a bending tester (ZBT-200, Z-tec). An ITO/PEN film ($R_s = 15 \text{ } \Omega/\text{sq}$) was purchased from Peccell technologies. The AgNWs TCE ($R_s = 15 \text{ } \Omega/\text{sq}$) was prepared by spin coating of AgNWs ink. The bending radius and speed for mechanical flexibility tests were 7.5 mm and 30 mm/sec, respectively. The sheet resistance of ITO/PEN and AgNWs/PEN TCEs were measured with a 4-point probe sheet resistance measurement instrument (MCP-T610, Mitsubishi Chemical).

Patterning of AgNWs TCEs using a photolithographic process

The AgNWs TCE was patterned using a photolithographic process for fabrication of OLED devices. First, positive photoresist (PR) was spin-coated onto the AgNWs films under the condition of 500 rpm (40 sec) followed by soft bake at $100 \text{ }^\circ\text{C}$ for 90 sec. Then, the positive-PR thin film was subjected to UV exposure for 2 sec, developed in aqueous tetramethylammonium hydroxide (90 sec), washed with deionized water, and baked at $120 \text{ }^\circ\text{C}$ for 2 min. The non-patterned area of AgNWs TCE was then etched by dipping in an etchant solution for 2 min and washed with deionized water. Then, the remaining positive PR was stripped by using propylene glycol monomethyl ether acetate (PGMEA). We checked the patterns of AgNWs TCE with optical microscope after develop and strip process.

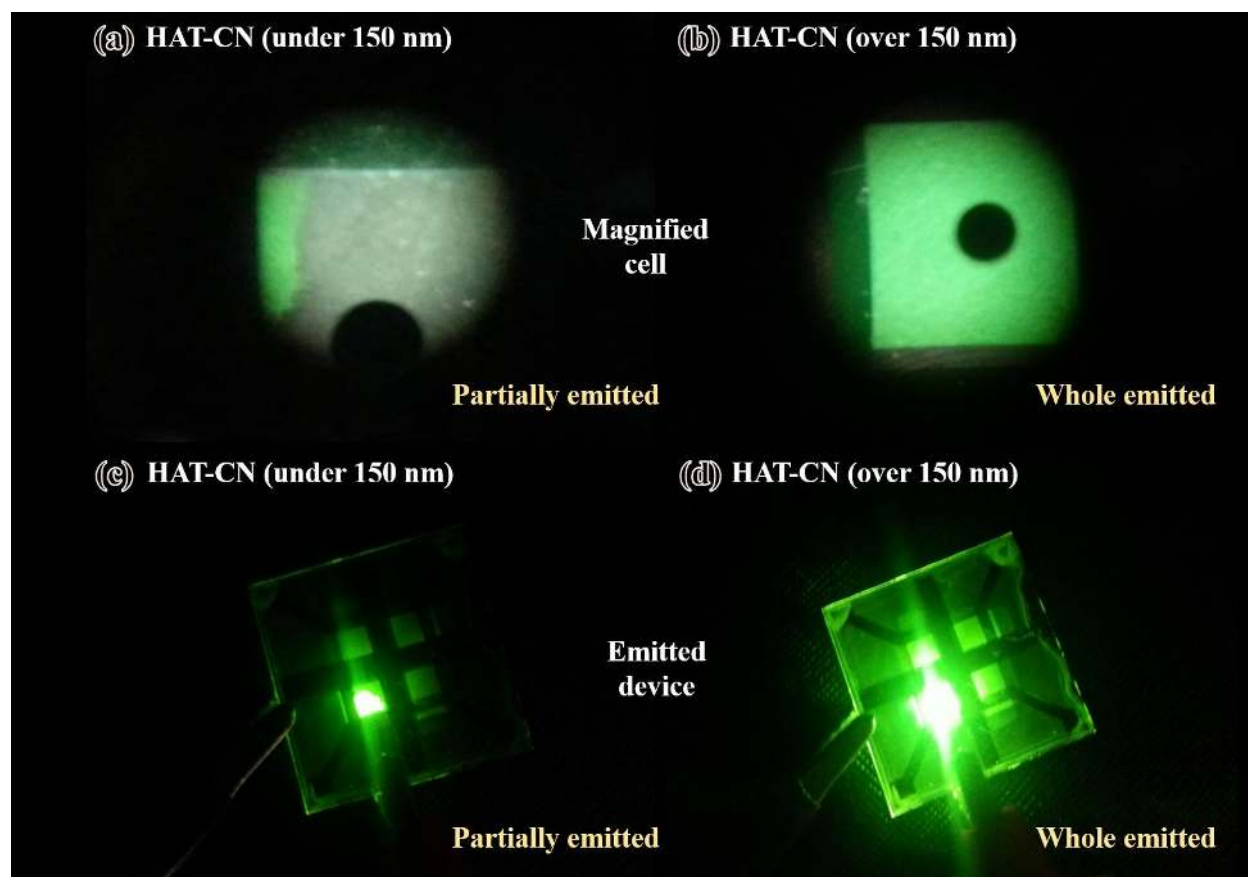


Fig. S2 Electroluminescence from PHOLEDs with different film thickness of HAT-CN HIL on the AgNWs TCE.

Fabrication of green phosphorescent organic light-emitting diodes (PHOLEDs) with AgNWs and ITO TCEs.

Patterned TCEs such as AgNWs and ITO were loaded on the tray and the tray was placed into the loading chamber of a cluster type OLED manufacturing system. All of materials were deposited by thermal evaporation with shadow masks. The shadow masks and tray were moved by robot arms in the cluster type manufacturing system. Therefore, we fabricated the green phosphorescence OLEDs with the TCE in high vacuum without venting the chamber. In addition, the deposition rates and doping concentrations of materials were controlled and measured using calibrated thickness monitors. In details, 1,4,5,8,9,11-hexaazatriphenylene-hexacarbonitrile (HAT-CN) and N,N'-diphenyl-N,N'-bis[4-(phenyl-m-tolyl-amino)phenyl]-biphenyl-4,4'-diamine (DNTPD) were deposited as hole injection layer (HIL). The deposition rate of HIL was about 1 Å/s. The deposition rates of N,N'-Di(naphthalene-1-yl)-N,N'-disphenyl-benzidine (α -NPB), Bathocuproine (BCP), and Tris(8-hydroxy-quinolato)aluminium (Alq₃) were also 0.1 Å/s. The dopant concentration in 4,4'-N,N'-dicarbazole-biphenyl (CBP) was controlled by changing deposition rate of fac-tris(2-phenylpyridine) iridium (Ir(ppy)₃). Lithium fluoride (LiF) and aluminum (Al) were deposited under 5×10^{-7} torr in a metal chamber at deposition rate of 0.1 and 1 Å/s, respectively. The device structure of the fabricated PHOLED is as follows: AgNWs or ITO TCE/HAT-CN (various thickness)/ α -NPB (40 nm)/10 wt% [Ir(ppy)₃] doped CBP (20 nm)/ BCP (20 nm)/ Alq₃ (40 nm)/LiF (1 nm)/Al (120 nm). The active area of the PHOLEDs was 3 x 3 mm². The fabricated PHOLEDs were transferred from the loadlock vacuum chamber into a nitrogen-filled glove box for encapsulation before measurement. The fabricated PHOLEDs were encapsulated with a glass cap and a UV-curable epoxy resin (Nagase XNR 5570).

Device characterization of PHOLEDs

All measurements were carried out under ambient condition at room temperature. The current density – voltage – luminance (J – V – L) and electroluminescence spectra of the fabricated PHOLEDs were measured using a Keithley 2400 programmable source meter and a Spectra Scan PR650 (Photo Research), respectively.

Table S1 Summary of relevant literature reporting AgNWs used OLEDs and PLEDs including our work reported in this article. Device type, Turn-on Voltage, Emitter and efficiencies are shown.

Previous Literature	Device Type	Turn-on Voltage [V]	Emitter	Current Efficiency [cdA ⁻¹]	Power Efficiency [lmW ⁻¹]
S1	OLED	5	White	49.0 ^a	30.3 ^a
S2	PLED	6.8	Green-yellow	11.4 ^b	-
S3	PLED	2.3	Green, fluorescent	14.0 ^c	-
S4	PLED	5.7	Phosphorescent (Blue, Green, Red)	21.5 (Blue) ^c	7.1 (Blue)
				39.3 (Green) ^c	9.6 (Green)
				8,8 (Red) ^c	1.7 (Red)
S5	PLED	12<	White (3 color, phosphorescent)	42.3 ^c	10.3 ^b
S6	OLED	6.6	Green, fluorescent	-	2.43 ^b
S7	PLED	7	White	4.0 ^b	-
S8	PLED	-	Orange-red	-	-
This work	OLED	3.9	Green, phosphorescent	44.5 ^c	35.8 ^b

^a at 1000 cdm⁻², ^b emitting both side, ^c Maximum value

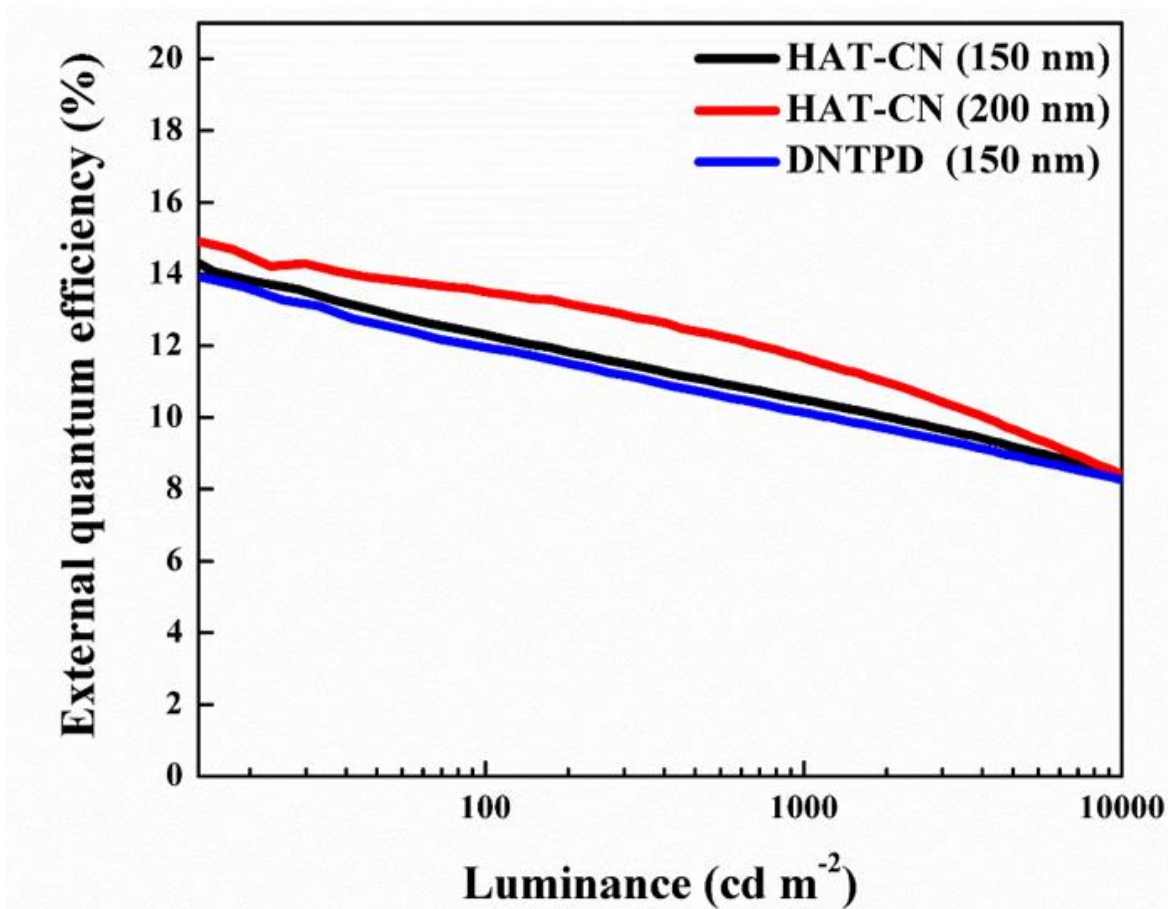


Fig. S3 External quantum efficiency of PHOLEDs with different film thickness of the HAT-CN and DNTPD HILs on the AgNWs TCE.

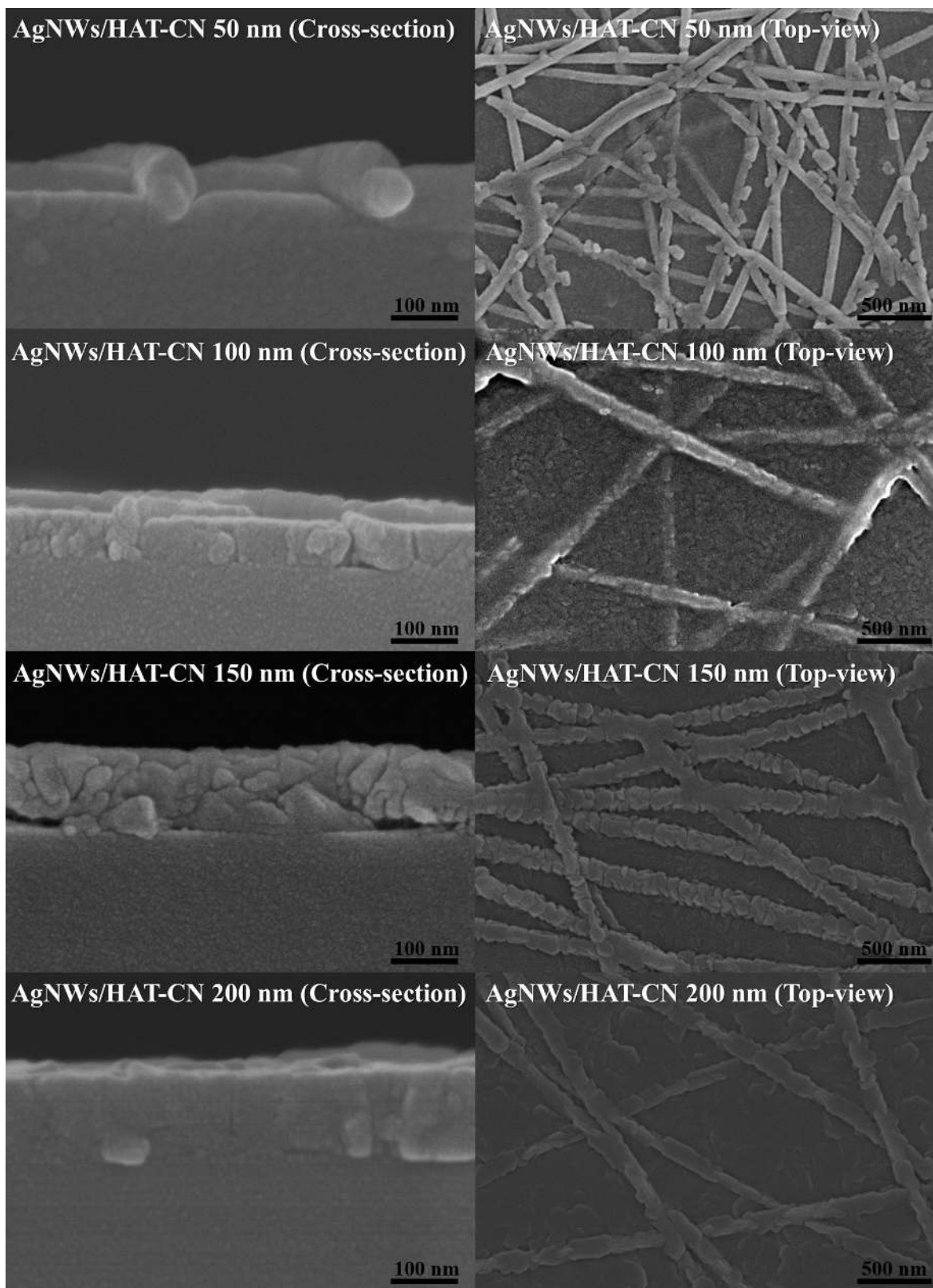


Fig. S4 SEM images of HAT-CN films with different thickness on the AgNWs TCE.

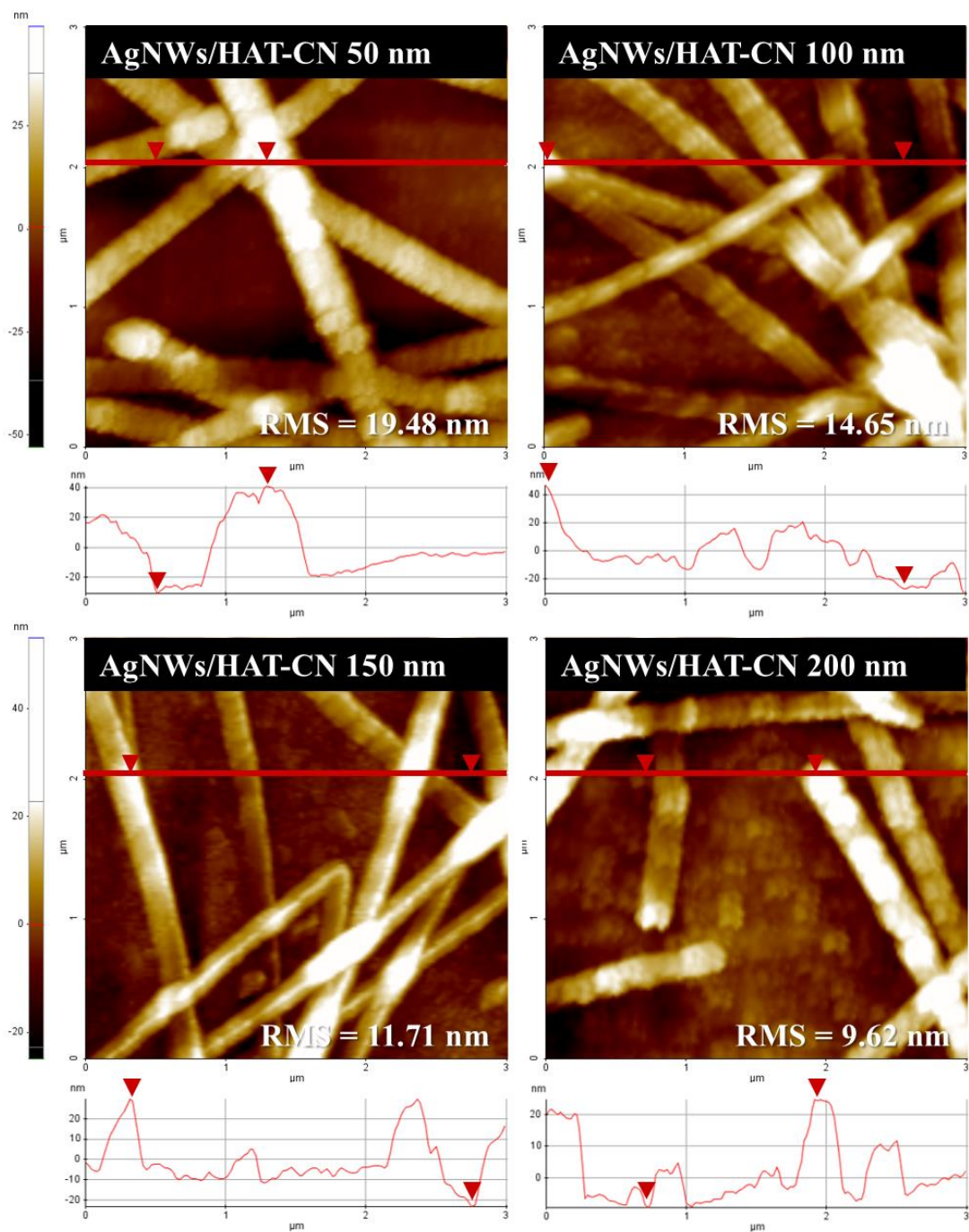


Fig. S5 AFM topographies of HAT-CN films with different thickness on the AgNWs TCE.

The surface morphology of HAT-CN films with different thickness on the AgNWs TCE was measured by using atomic force microscope (NX10, Park systems).

Ultraviolet Photoelectron Spectroscopy (UPS) Measurements of AgNWs and AgNWs/HAT-CN TCEs

A AgNWs TCE on a cleaned glass substrate was placed in ultra-high vacuum chamber for deposition of HAT-CN. Then, HAT-CN was deposited onto the AgNWs TCE by thermal evaporation at ultra-high vacuum (5×10^{-7} torr). Deposition of HAT-CN was controlled at speed of 1 Å/s using calibrated thickness monitors. The film thickness of HAT-CN on the AgNWs TCE was 1.2 nm. The UPS measurements of AgNWs and AgNWs/HAT-CN TCEs were carried out in a Ultra Spectrometer (ESCALAB 250Xi, Thermo Scientific) using a He I (21.2 eV) discharge lamp. The work functions (Φ) of both TCEs were calculated from the onset of the secondary edge (E_{SE}) using the equation ($\Phi = 21.2 - E_{SE}$) with sample bias.

Mechanical flexibility test of the PHOLEDs with AgNWs/PEN and ITO/PEN TCEs

We performed the bending test of the PHOLEDs with AgNWs and ITO TCEs under ambient condition without encapsulation. The device operation voltage and initial luminous intensity of a PHOLED with the AgNWs/PEN or ITO/PEN TCEs were 6V and 500 cd/m². Then, each PHOLED was rolled around bending radius of 7.5 mm, subsequently unrolled. The luminous intensity of each PHOLED was compared to its initial value.

Table S2. Device characteristics of a flexible PHOLED with AgNWs/PEN TCE and HAT-CN HIL (200 nm).

TCE	HAT-CN Thickness [nm]	Turn-on voltage [V]	Max CE [cd/A]	Max PE [lm/W]	Voltage at Max Luminance [V]	Max Luminance [cd/m ²]
AgNWs/PEN	200	3.9	41.1	32.8	11.0	60310
ITO/PEN	200	3.9	43.1	33.5	13.4	33800

(CE = current efficiency, PE = power efficiency)

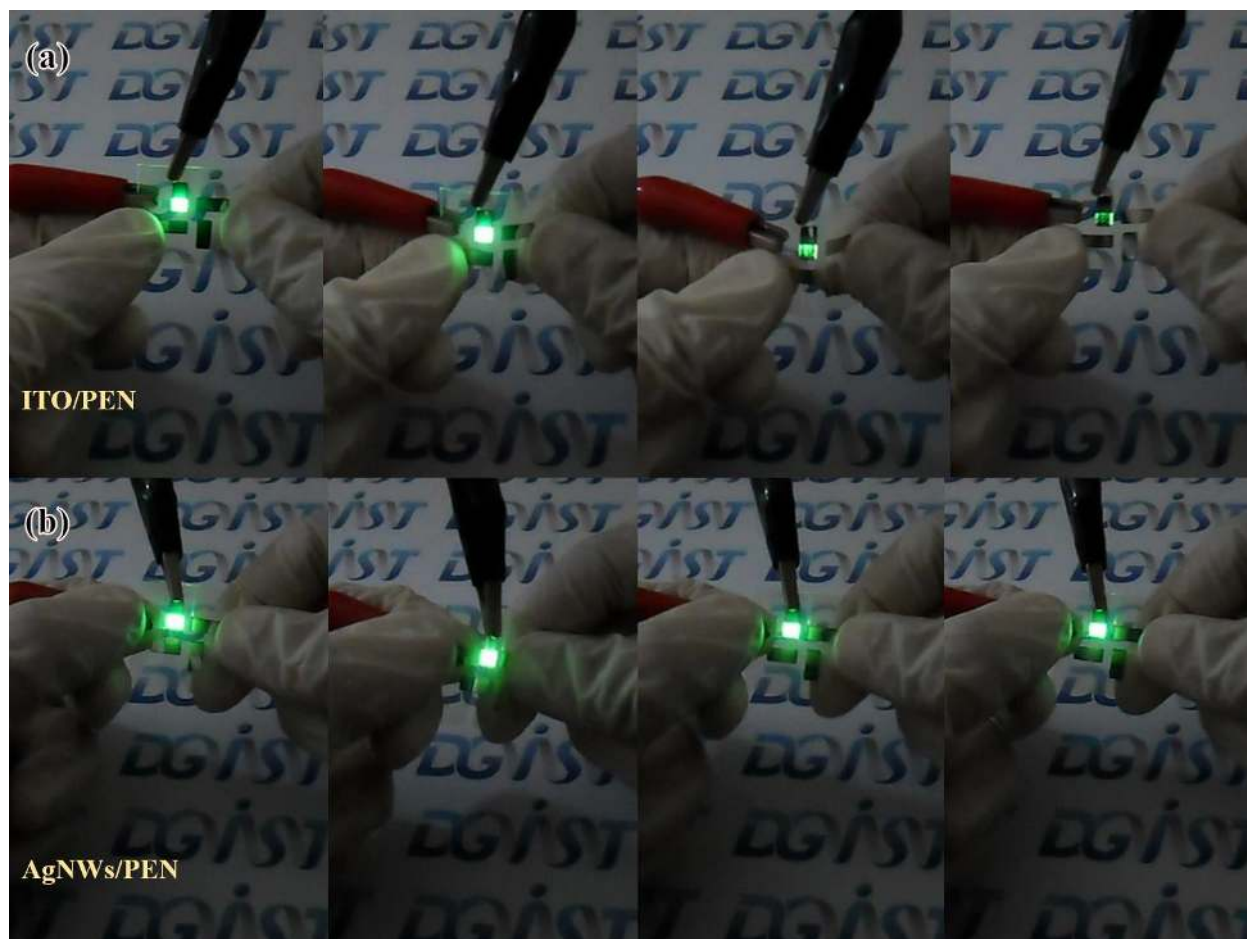


Fig. S6 Mechanical flexibility test of flexible PHOLEDs with (a) ITO/PEN and (b) AgNWs/PEN TCEs.

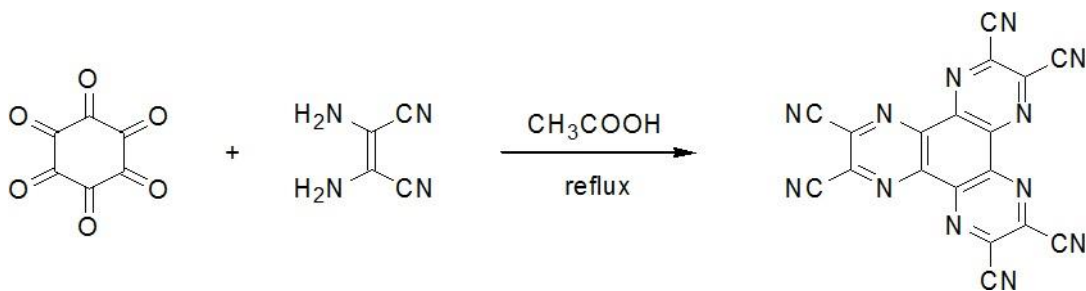
Materials

Synthesis of 1,4,5,8,9,11-hexaazatriphenylenehexacarbonitrile (HAT-CN)

Hexaketocyclohexane octahydrate and diaminomaleonitrile were purchased from sigma aldrich. Then, HAT-CN compound was synthesized as shown in Scheme 1.

Hexaketocyclohexane octahydrate (1.0 g, 5.0 mmol) and diaminomaleonitrile (1.78 g, 16.5 mmol) were added to acetic acid (CH₃COOH) (50 ml) and then the solution was refluxed for 72 h. Then, hot black suspension was filtered off and washed with deionized water to afford a black solid. The solid was dried in vacuum and purified by vacuum gradient sublimation to afford pure HAT-CN.

Scheme 1 Synthesis of 1,4,5,8,9,11-hexaazatriphenylenehexacarbonitrile (HAT-CN).



Other materials

The sublimated grade of N,N'-diphenyl-N,N'-bis[4-(phenyl-m-tolyl-amino)phenyl]-biphenyl-4,4'-diamine (DNTPD) was purchased from Luminescence Technology and was used for the hole injection layer (HIL). The sublimated grade of N,N'-di(naphthalene-1-yl)-N,N'-disphenylbenzidine (α -NPB) was purchased from eRay and used for the hole transport layer (HTL). The sublimated grade of fac-tris(2-phenylpyridine) iridium [Ir(ppy)₃] and 4,4'-N,N'-dicarbazole-biphenyl (CBP) were purchased from eRay and used for the emitting layer (EML). The sublimated grade of bathocuproine (BCP) was purchased from Luminescence Technology and used for hole blocking layer (HBL). The sublimated grade of tris(8-hydroxyquinolino)aluminium (Alq₃) was purchased from Luminescence Technology and was used for the electron transport layer (ETL).

REFERENCES

- S1 W. Gaynor, S. Hofmann, M. G. Christoforo, C. Sachse, S. Mehra, A. Salleo, M. D. McGehee, M. C. Gather, B. Lüssem and L. Müller-Meskamp, *Adv. Mater.*, 2013, **25**, 4006-4013.
- S2 J. Liang, L. Li, X. Niu, Z. Yu and Q. Pei, *Nat. Photon.*, 2013, **7**, 817-824.
- S3 Z. Yu, Q. Zhang, L. Li, Q. Chen, X. Niu, J. Liu and Q. Pei, *Adv. Mater.*, 2011, **23**, 664-668.
- S4 L. Li, Z. Yu, W. Hu, C. h. Chang, Q. Chen and Q. Pei, *Adv. Mater.*, 2011, **23**, 5563-5567.
- S5 L. Li, Z. Yu, C.-h. Chang, W. Hu, X. Niu, Q. Chen and Q. Pei, *Phys. Chem. Chem. Phys.*, 2012, **14**, 14249-14254.
- S6 X. Y. Zeng, Q. K. Zhang, R. M. Yu and C. Z. Lu, *Adv. Mater.*, 2010, **22**, 4484-4488.
- S7 J. Liang, L. Li, K. Tong, Z. Ren, W. Hu, X. Niu, Y. Chen and Q. Pei, *ACS Nano*, 2014, **8**, 1590-1600.
- S8 S. Coskun, E. S. Ates and H. E. Unalan, *Nanotechnology*, 2013, **24**, 125202.